

The following manuscript entitled “Extrinsic lactose fines improve dry powder inhaler formulation performance of a cohesive batch of budesonide via agglomerate formation and consequential co-deposition“ has been published in International Journal of Pharmaceutics, Volume 478, Issue 1, 15 January 2015, Pages 53–59.

DOI: 10.1016/j.ijpharm.2014.11.019

Copyedited version can be downloaded at
<http://www.sciencedirect.com/science/article/pii/S0378517314008229>

Extrinsic lactose fines improve dry powder inhaler formulation performance of a cohesive batch of budesonide via agglomerate formation and consequential co-deposition

Hanne Kinnunen^{1,2*}, Gerald Hebbink³, Harry Peters³, Deborah Huck⁴, Lisa Makein⁴ and Robert Price¹

¹ Pharmaceutical Surface Science Research Group, Department of Pharmacy and Pharmacology, University of Bath, BA2 7AY, Bath, UK

² Current affiliations: School of Medicine, Pharmacy and Health, and Wolfson Research Institute. Durham University, Queen's Campus, Stockton on Tees, TS17 6BH, UK.

³ DFE Pharma, Klever Strasse 187, 47574 Goch, Germany.

⁴ Malvern Instruments Ltd, Enigma Business Park, Grovewood Road, WR14 1XZ, Malvern, UK

***Corresponding author:**

Dr Hanne Kinnunen

Telephone: +44 (0) 191 334 0400

E-mail: hanne.kinnunen@durham.ac.uk

Abstract

The aim of the study was to investigate how the fine particle content of lactose carriers prepared with different types of lactose fines regulates dry powder inhaler (DPI) formulation performance of a cohesive batch of micronised budesonide. Budesonide formulations (0.8 wt-%) were prepared with three different lactose carriers (Lactohale (LH) LH100, 20 wt-% LH210 in LH100 and 20 wt-% LH300 in LH100). Fine particle fraction of emitted dose (FPF_{ED}) and mean mass aerodynamic diameter (MMAD) of budesonide was assessed with a Next Generation Impactor (NGI) using a Cyclohaler at 90 l/min. Morphological and chemical characteristics of particles deposited on Stage 2 were determined using a Malvern Morphologi G3-ID. The results indicate that increasing concentration of lactose fines (<4.5 µm) not only increased the FPF_{ED} but also the MMAD of budesonide, suggesting drug deposition in agglomerates. Presence of agglomerates on Stage 2 was confirmed by morphological analysis of particles. Raman analysis of material collected on Stage 2 indicated that the more fine lactose particles were available the more agglomerates of budesonide and lactose were delivered to the Stage 2. These results suggest drug-fines agglomerate formation is an important mechanism for how lactose fines improve and regulate DPI formulation performance.

Keywords: Lactose, dry powder inhaler, Raman spectroscopy

1. Introduction

In dry powder inhaler (DPI) formulations, drug particles with aerodynamic diameters of less than 5 μm are required to target the conducting airways. The particle size is conventionally achieved by secondary processing of crystalline drug using energy intensive air-jet micronisation (Chan, 2006). However, due to the high interparticle forces in micronised, cohesive Geldart type C (Geldart, 1973) powders, and low doses required for drug delivery to the lungs, metering of and fluidising a drug only dose is onerous. Thus, to allow adequate metering and increased flowability of the powder, the micronised drug is commonly formulated with coarser, fluidisable Geldart type A (Geldart, 1973) carrier particles. The carrier of choice for DPI formulations is most often alpha lactose monohydrate.

Historically, a vast number of studies, reviewed by Jones and Price (2006), have shown that the presence of fine lactose particles in a DPI formulation improves the formulation performance in terms of delivered dose. As a general rule, therefore, in addition to the drug and the coarse carrier, fine particle lactose is often present in DPI formulations, either as an extrinsic added fraction of fines or as intrinsic fines within the coarse carrier. However, to date, the exact mechanism for how these fine lactose particles alter the formulation performance has remained unclear, with active sites (El-Sabawi et al., 2006; Ganderton, 1992; Young et al., 2005), drug-lactose fine agglomerate formation (Lucas et al., 1998), and increased cohesion (Shur et al., 2008) theories attempting to explain the phenomenon. Due to the shortcomings of each of these theories, more recently it has also been suggested that all these three theories may be at play simultaneously (Grasmeijer et al., 2014). The concept of total fines, which also takes the concentration of the drug in the formulation into

account when defining fines, has also been introduced as an explanation for the improved performance in the presence of a fine particle component (Thalberg et al., 2012). It has also been suggested that a more favourable powder microstructure for deagglomeration may be achieved by adding lactose fines (Behara et al., 2011).

As required by the regulatory authorities, cascade impactors are routinely used for assessing the DPI formulation performance (European Medicines Agency, 2007). Traditionally, the drug content in the different parts of the impactor is assayed by solution chemistry based techniques. However, some studies have also made an attempt of understanding the mechanisms by which the lactose fines govern the DPI performance by determining the deposition of lactose in the different parts of the impactor alongside the drug determination (Guchardi et al., 2008; Karhu et al., 2000; Srichana et al., 1998b). These studies proved that in addition to the drug, also fine lactose is deposited on the impactor stages. However, due to the limitations of the traditional solution chemistry based analytical techniques, these studies only provided speculative evidence of agglomerate formation between the lactose fines and the drug. Therefore, to study the possible co-deposition of the drug and lactose fines, there remains a need for discovering novel characterisation methods to probe the possible interactions between the lactose fines and drug particles upon deposition.

Combination of the scanning electron microscopy and X-ray microanalysis has been used for studying the interactions between lactose and salbutamol sulphate particles (Srichana et al. 1998a). More recently, Raman spectroscopy has emerged as a promising technique for studying particulate interactions especially in combination

pressurised metered dose (pMDI) formulations (Rogueda et al., 2011; Steele et al., 2004; Theophilus et al., 2006). However, also studies where DPI products have been investigated using Raman spectroscopy have been published (Kinnunen et al. 2009, Šašić and Harding, 2010). Both the studies concluded that Raman spectroscopy was a promising technique for studying deposition patterns of DPI formulation components. However, both these studies only demonstrated the capability of Raman spectroscopy in analysing particulate interactions taking place in DPI formulations and were limited in their experimental approach due to low number of particles analysed. Following recent developments in instrumentation, the next step for gaining statistically significant data was taken in the current study as morphologically directed Raman spectroscopy was used for characterising the morphological properties and chemical composition of the material delivered to the impactor stages in parallel with traditional *in vitro* performance assay of the formulations.

The aim of the current study was to investigate the drug deposition in the Next Generation Impactor from DPI formulations containing different amounts and types of extrinsic lactose fines in greater detail using morphologically directed Raman spectroscopy (MDRS) in parallel with *in vitro* performance assessment of the formulations. Particular emphasis of the study was on investigating and quantifying the extent of possible agglomerate formation and co-deposition of lactose fines and a model drug, micronised budesonide, and how this influences the formulation performance as a whole. This was done to enhance the understanding of the mechanisms governing drug delivery from DPI formulations containing fine particle lactose.

2 Materials and methods

2.1 Materials

Lactohale products, namely a coarse, sieved grade of lactose Lactohale[®]100, micronised grade Lactohale[®]300 and a milled grade Lactohale[®]210 (Hereafter designated as LH100, LH300 and LH210, respectively), were all donated by DFE Pharma (Goch, Germany). Micronised budesonide with particle size within the respirable range ($d_{90}=4.40\ \mu\text{m}$) and a cohesive-adhesive balance (CAB) value of 0.62 (Kinnunen et al., 2014) was received from Sterling S.r.l (Perugia, Italy).

Water used during the study was reverse osmosis purified (Merck Millipore, Darmstadt, Germany). Acetonitrile and methanol were purchased from Sigma Aldrich (Gillingham, UK) and were of HPLC quality.

2.2 Preparation of lactose pre-blends

The fine grades of lactose (LH300 and LH210) were blended with the coarse grade of lactose (LH100) at 20 wt-% concentration. Briefly, 20 g of the fine lactose was sandwiched between 80 g of LH100 in two layers in a stainless steel vessel with a volume of $500\ \text{cm}^3$. The headspace within the vessel was approximately 1/3 of the volume of the vessel. Turbula (Glen Creston, Middlesex, UK) blending at 46 rpm was applied for 60 minutes after which the pre-blends were passed through $850\ \mu\text{m}$ aperture sieve to break up any large agglomerates. The pre-blends were stored at $20 \pm 2\ ^\circ\text{C}$ and 44% relative humidity (RH) for at least 24 hours before any further work was performed.

2.3 Particle sizing of the lactose carriers

The particle size distributions of the lactose carriers were characterised using a Sympatec Helos laser diffraction system equipped with R4 lens and controlled by Windox X software (both from Sympatec, Clausthal-Zellerfeld, Germany). The Helos dry dispersion system with the disperser pressure set to 2 bar was used for introducing the powder into the measurement zone in conjunction with Vibri powder feeder with a feed rate of 30% and gap width of 2 mm. The background scattering was recorded for 10 seconds after which five repeated measurements of 5 seconds duration were recorded for each of the samples with the optical concentration threshold set to 0.5%. High resolution laser diffraction (HRLD) model of the Windox software was used for converting the raw scattering data into particle size distributions.

2.4 Preparation of model DPI formulations

Model DPI formulations were prepared with micronised budesonide at 0.8 wt-% concentration in quantities of 40 g. The CAB value of the budesonide (0.62) meant that the drug is adhesive to the lactose and therefore low shear Turbula blending could be used for obtaining a uniform blend between the lactose carrier and the drug particles. Briefly, budesonide was sandwiched between half of the lactose and blended with a Turbula in a stainless steel vessel of 500 cm³ volume for 10 minutes at 46 rpm. The remaining lactose was then added and further 45 minutes of blending was applied. The blends were subsequently passed through a 250 µm aperture sieve and stored at 20 ± 2 °C and 44% RH for at least 24 hours before any further work was carried out. To ensure that the dose variation was below 6%, the content

uniformity of the blends was assessed by taking ten aliquots of 12.5 mg from different parts of the formulation and assaying the drug content within the aliquots.

2.5 *In vitro* assessment of formulation performance

Size 3 hydroxypropylmethylcellulose (HPMC) capsules (Qualicaps, Spain) were manually filled with 12.5 mg of the formulations. A Cyclohaler device (Teva Pharmaceuticals, The Netherlands) was used for aerosolising the formulations into a Next Generation Impactor (NGI, Copley Scientific, Nottingham, UK) equipped with a pre-separator. Air was drawn through the impactor at 90 l/min for 2.7 seconds (Kubavat et al., 2012) as controlled by a TPK critical flow controller (also from Copley Scientific). Two capsules were aerosolised into the impactor with plates coated with silicone oil and the pre-separator filled with 15 ml of mobile phase. The drug collected in the different parts of the impactor was dissolved in mobile phase and the drug content assayed by high performance liquid chromatography (HPLC).

The mean mass aerodynamic diameter (MMAD) and fine particle fraction (<5 µm) of budesonide were calculated from the cumulative impactor stage-by-stage deposition data as instructed by the Pharmacopoeia (EMA, 2007). The fine particle fraction of emitted dose (FPF_{ED}) is defined as the ratio between the fine particle mass and the dose of the drug recovered after the capsule and device.

2.6 High performance chromatography (HPLC) assay of budesonide

The concentration of budesonide collected in the different parts of the impactor was assessed using high performance liquid chromatography (HPLC) following a method reported elsewhere (Kubavat et al., 2012). Briefly, the samples were dissolved in

mobile phase consisting of 20% water, 35% acetonitrile and 45% methanol. The flow rate through the HPLC system was set to 1.5 ml/min using a PU-980 pump (Jasco, Tokyo, Japan). Aliquots of 100 μ l of volume were injected into a 250 mm long Hypersil-ODS column with an inner diameter of 4.6mm and packing material particle size of 5 μ m (Thermo Scientific, Loughborough, UK) using an AS-950 autosampler (Jasco, Tokyo, Japan). The column oven CO-965 (Jasco, Tokyo, Japan) temperature was set to 40°C and wavelength of 244 nm was used for detecting budesonide on a UV-975 detector (Jasco, Tokyo, Japan). The peak eluted at 3.75 min.

2.7 Morphological and chemical characterisation of material deposited in the Next Generation Impactor

A mirror surfaced microscope slide was placed underneath the nozzles on Stage 2 of the NGI to collect sample of deposited material from each of the formulations under investigation. The morphological properties of the collected particles were characterised on the Morphologi G3-ID morphologically directed Raman system (Malvern Instruments, Worcestershire, UK). Episcopic bright field illumination was used for the microscopic visualisation of the particles with the light intensity calibrated to 80.0 ± 0.2 %. The samples were scanned using the 50x objective lens with the focus fixed at 0 μ m and the plate tilt compensation enabled. The scan area size was set to 4.5 mm by 4.5 mm, the overlap between any two adjacent frames to 40%, the binary threshold to a grayscale value of 130 and the trash size to 10 pixels. Post analysis, any touching particles were removed by filtering out particles with values of solidities below 0.92. Before the shape analysis, particles consisting of less than 100 pixels were filtered out to remove noise from the shape distributions.

After the morphological analysis of particles deposited on Stage 2, the particles were sorted according to their size using circular equivalent (CE) diameter. All the particles larger than 3 μm were highlighted for the Raman analysis that was performed using the Kaiser Optical Systems MK II Probe head integrated in the Morphologi G3-ID system. The XY coordinates of the particles recorded during the morphological analysis were used for locating the centre of mass the particles, where the Raman spectrum was acquired. The Raman spectrum for each of the particles was collected using 10 seconds exposure time with excitation at a wavelength of 785 nm over the spectral range of 100 to 1825 cm^{-1} at a resolution of 4 cm^{-1} . The signal was detected using a charge coupled device (CCD) camera. The Raman spot size with the 50x objective was approximately 3 μm in diameter.

Reference Raman spectra, which were used for identifying the chemical composition of the material collected on Stage 2, were recorded for pure lactose and pure budesonide. The identification was performed by comparing the entire spectrum for each of the analysed particles to the library spectra of lactose and budesonide using the Morphologi G3-ID software by allocating matching scores for lactose and budesonide for the particles analysed with regards to the similarity of the spectra to the library spectra of lactose and budesonide. Matching score of 1 indicates identical spectra and score of 0 indicates the spectrum bears no resemblance to the library spectra at all. On the basis of the scores, the particles were classified as pure lactose (Lactose ≥ 0.75 and budesonide < 0.45), pure budesonide (Budesonide ≥ 0.75 and lactose < 0.45) or an agglomerate of lactose and budesonide (All the remaining particles). When allocating the classification parameters for the pure

substances, visual comparison of the library spectra and the spectra of the particles was used for confirming that no obvious signals of the other component were seen in the spectra. Similarly, for the particles classified as agglomerates, it was visually inspected that the characteristic signals for both the pure substances were present in the spectra.

3 Results and discussion

3.1 Particle size of the carriers

The fines content ($\%<4.5\ \mu\text{m}$) of the lactose carriers investigated in the current study are summarised in Table I. The proportion of fine particle lactose in the carriers ($\%<4.5\ \mu\text{m}$) increased from 1.3% for the LH100 only to 6% for the 20% LH210 blend and 23% for the 20% LH300 blend.

3.2 *In vitro* performance of the formulations

Table I illustrates that the fine particle fraction of emitted dose (FPF_{ED}) for the formulations increased from approximately 24 to 26 to 40% for LH100, 20 wt-% LH210 blend and 20% LH300 blend, correspondingly. This is in an agreement with previous studies (Guenette et al., 2009; Louey et al., 2003) where it was shown that an increase in the proportion of fine lactose particles present in the carrier improved the DPI formulation performance. Notably, Table I shows that simultaneously with improving FPF_{ED} , the mean mass aerodynamic diameter (MMAD) of budesonide also increased. The increase in the MMAD indicated that the drug was delivered to the impactor stages in larger entities upon the increase

in the lactose fines content. These could either be agglomerated drug particles or agglomerates of the fine lactose and the drug particles.

The stage-by-stage deposition profiles of the drug aerosolised from the different formulations are presented in Figure 1. The amount of drug retained in the capsules was lower for the 20% LH300 formulation than for the LH100 only and 20% LH210 formulations but the device deposition remained somewhat constant for the three different formulations. An increase in the mouthpiece and throat deposition was observed upon increasing the lactose fines content of the formulations (LH100 < 20% LH210 blend < 20% LH300 blend). The pre-separator deposition drastically decreased upon increasing the fines content of the carrier, and the decrease here was reflected in the amount of drug delivered to the impactor stages, which generally speaking increased upon the increase in the fines concentration. The increase was significant ($p < 0.05$) on all the stages for LH300 formulation and on stages 1 and 2 for LH210 formulation compared to the formulation containing LH100 only. These data are in an agreement with numerous previous studies where it has been shown that the increasing lactose fines content of a carrier results in decreased pre-separator deposition and increased drug delivery to the impactor stages (Louey et al., 2003; Louey and Stewart, 2002; Srichana et al., 1998b; Steckel et al., 2006).

3.3 Morphological and chemical characteristics of material deposited on Stage 2

The number based and volume converted circular equivalent (CE) diameter distributions of the material collected on the NGI Stage 2 from the different formulations are summarised in Table II. In number terms, a slight increase in the

value of d10 from 1.56 to 1.86 μm was seen as the fines content of the formulations was increased. The cut-off diameter of Stage 2 when the NGI is operated at 90 l/min is 3.61 μm (Marple et al., 2003). Table II shows that the number based values of d50 measured for the formulations were close to this at 3.62 to 3.94 μm . Values of d50 did not exhibit a clear trend related to the fines content of the formulations. In terms of d90, an increase from 5.77 to 6.72 μm was apparent as the fines content increased. The increasing particle size in the upper end of the distributions as the fines content was increased is clearly visible in Figure 2A, where the number based CE diameter distributions of the material collected on Stage 2 from the different formulations are presented. Table II and Figure 2B, where the volume converted CE diameter distributions of the material collected on Stage 2 are shown, indicate that in volume terms, the increase in the particle size at the upper end of the distributions was even more pronounced with d90 increasing from 8.06 to 10.4 μm . These data suggest the material collected on Stage 2 became increasingly agglomerated upon increasing lactose fines content of the formulation.

Particle shape of the material collected from Stage 2 is summarised in Table II in terms of mean high sensitivity (HS) circularity and convexity values for the different formulations. In case of both the shape descriptors, a decreasing trend in the mean values was seen as the lactose fines concentration of the formulations was increased. Following the definition of these shape parameters (Willen, 2008), the higher the value of the parameters, the more compact the shape of a particle. It is also known that agglomerates often exhibit less compact shape than primary particles (Huck, 2007). Therefore, the decreasing trend in the particle shape descriptors upon the addition of fines indicated an increased presence of

agglomerates. The increasing degree of agglomeration in the presence of lactose fines, as indicated by the larger particle size and less compact shape, is in an agreement with the increase observed in MMAD of the drug aerosolised from the formulations upon addition of the fines, as was shown in Table I, and coincide with improved formulation performance. Therefore, these data suggest that agglomerate formation and/or co-deposition play an important role in increasing DPI formulation performance.

To further investigate the possible agglomerate formation and co-deposition between budesonide and lactose fines, a novel approach of Raman analysis of significant number of particles collected on Stage 2 was taken. A 50x magnification field of view photomicrograph of material deposited on Stage 2 from the 20% LH300 formulation is presented in Figure 3. The photomicrograph clearly demonstrates that both primary and agglomerated particles were collected on Stage 2. The Raman spectroscopic characterisation enabled the analysis of the chemical components forming these agglomerates. The Raman spectrum of the highlighted particle is displayed on the top right of Figure 3 and the library spectra of lactose and budesonide below that. The characteristic, strong signal of budesonide at 1656 cm^{-1} , deriving from the stretching vibration of C=C bond in the aromatic ring of the steroid backbone of the molecule (Ali et al., 2007), is present in the spectrum of the highlighted particle. Also the fingerprint for the glycosidic bond of lactose between the wavenumbers of 300 and 500 cm^{-1} (Susi and Ard, 1974) is exhibited in the spectrum of the highlighted particle. The matching scores for the library spectra as allocated by the Morphologi G3-ID software for this particle were 0.681 for lactose and 0.635 for budesonide. Therefore, based on the matching scores and the visual

inspection of the Raman spectrum, the highlighted particle could be identified as an agglomerate of lactose and budesonide. Similarly, primary particles of lactose and budesonide could be characterised based on their Raman spectrum. This way, the chemical composition of 1353 (LH100), 1095 (+20% LH210) and 1156 (+20% LH300) particles collected on Stage 2 were characterised for the formulations.

Following the Raman spectroscopic fingerprinting of the particles collected on Stage 2, a classification was set up according to whether the material was lactose, budesonide or an agglomerate of the two components. Proportions of the different chemical species in the different formulations are summarised in Table III. These data show that, even for the formulation prepared with LH100 only, nearly 40% of the particles delivered to the impactor Stage 2 were lactose. With added lactose fines, the proportion of lactose delivered to the Stage 2 was even higher at approximately 80%. These data are in an agreement with previous studies, where it was reported that fine particle lactose is indeed delivered to the impactor stages (Guchardi et al., 2008; Karhu et al., 2000; Srichana et al., 1998b).

Table III also demonstrates that the majority, nearly half, of the particles on Stage 2 from the LH100 only formulation were budesonide. In contrast, the proportion of pure budesonide in the formulations with added lactose fines was very low, with 10% for the 20% LH210 formulation and 6% for the 20% LH300 formulation characterised as pure budesonide.

Analysing the amounts of lactose and the drug particles delivered to the different parts of the impactor is straightforward by different chemical assays, and indeed has

been carried out in previous studies (Srichana et al., 1998a). However, while providing valuable information on co-deposition, these techniques cannot be used for addressing the possible presence of drug-lactose fine agglomerates. Using Raman spectroscopy for analysing the chemical composition of the particles collected on the impactor stages enables studying the possible agglomerate formation between two chemically different species. A previous study used Raman spectroscopy for qualitatively assessing the chemical composition of material deposited on the impactor stages (Kinnunen et al., 2009). The results showed co-deposition of lactose and drug took place. The next step was taken in the current study by quantifying the proportions of drug-lactose agglomerates delivered to the impactor stage. Table III demonstrates that, of all the particles deposited on Stage 2, the proportion of agglomerates of budesonide and lactose fines remained somewhat constant for all the formulations with the proportion varying between 11.5 and 17.0%.

To understand the underlying mechanisms for how the lactose fines alter the DPI performance, further analysis relating the *in vitro* deposition of the drug to the proportion of drug delivered to Stage 2 either as pure budesonide or agglomerates was performed. These data are summarised in Table IV. The total proportion of budesonide containing species (pure budesonide and agglomerates) was approximately 63% for the LH100 only formulation and approximately 20% for the formulations containing added lactose fines. Because the proportions of agglomerates and pure budesonide of the budesonide containing species were known (Table III), the amounts of budesonide in agglomerates and as pure budesonide could be quantified. This analysis revealed that interestingly, as shown in Table IV, the mass of the drug delivered on the Stage 2 of the impactor as pure

budesonide remained somewhat constant at between 2.2 and 2.6 μg from all the formulations. Meanwhile, the mass of budesonide delivered to the Stage 2 as agglomerates increased from 0.7 to 2.6 to 7.4 μg , respectively, as the lactose fines content of the formulations increased. For 20% LH210 formulation the mass of budesonide in agglomerates was approximately four times as high as for LH100 formulation. For 20% LH300 formulation, the mass of budesonide in agglomerates on Stage 2 was tenfold compared to the LH100 only formulation. Figure 4 clearly illustrates the increasing trend in the proportion of budesonide deposited as agglomerates with a decrease in the proportion of pure budesonide upon increasing lactose fines content of the carrier.

These data therefore demonstrate that agglomerate formation and co-deposition of lactose fines and a cohesive batch of micronised budesonide takes place upon the addition of lactose fines and consequentially, an improvement in the DPI performance is achieved. These results also indicate that the lactose fines have to be fine enough to be co-deposited in the impactor stages with the drug if an improvement in formulation performance is to be gained. Therefore, these results also explain why only the finest fractions of lactose fines are efficient in improving the DPI performance, as has been previously reported (Guenette et al., 2009; Louey et al., 2003)

4 Conclusions

A combination of *in vitro* testing, morphological analysis and Raman spectroscopy was used to investigate the mechanisms that govern fine particle deposition in carrier based DPIs. The *in vitro* analysis established an improvement in the fine

particle delivery and an increasing trend in MMAD upon increasing concentration of lactose fines present in the carrier. Morphological analysis of material deposited on Stage 2 demonstrated increasing particle size and less compact shape, both characteristic of agglomerate formation, upon increasing lactose fines content. By means of Raman spectroscopy, proportions of pure budesonide and lactose, and the agglomerates of the two materials delivered to Stage 2 could be quantified. The amount of budesonide-only particles on stage 2 was found to be constant for all three formulations, and an increasing amount of budesonide upon increasing lactose fines was observed. This was attributed to agglomerate formation between lactose fines and budesonide. Therefore, the results of this study compellingly demonstrate that agglomerate formation between drug and the lactose fines is very likely a dominating mechanism for how extrinsic lactose fines improve and regulate DPI performance. The more fines were available within the carrier, the more budesonide was agglomerated with the fines, and consequentially delivered to the impactor stage. The results also shed light to the question why only finest lactose fines are efficient in improving the DPI performance. This is because the lactose fines have to be fine enough to be co-deposited within the impactor with the drug particles. As a consequence, the results of the study highlighted why the proportion of fine particles present in the carrier is such a popular tool for predicting the DPI performance amongst the formulators.

Acknowledgements

DFE Pharma is acknowledged for funding the study. The authors are indebted to Dr Jag Shur for assistance in organising the parallel *in vitro* and morphologically

directed Raman experiments. Malvern instruments Ltd. are acknowledged for access to Morphologi G3-ID.

References

Ali, H.R.H., Edwards, H.G.M., Kendrick, J., Munshi, T., Scowen, I.J., 2007.

Vibrational spectroscopic study of budesonide. *Journal of Raman Spectroscopy* 38, 903-908.

Behara, S.R.B., Larson, I., Kippax, P., Morton, D.A.V., Stewart, P., 2011. An approach to characterising the cohesive behaviour of powders using a flow titration aerosolisation based methodology. *Chemical Engineering Science* 66, 1640-1648.

Chan, H.-K., 2006. Dry powder aerosol drug delivery--Opportunities for colloid and surface scientists. *Colloids and Surfaces A: Physicochemical and Engineering Aspects* 284-285, 50-55.

El-Sabawi, D., Edge, S., Price, R., Young, P.M., 2006. Continued investigation into the influence of loaded dose on the performance of dry powder inhalers: Surface smoothing effects. *Drug Development and Industrial Pharmacy* 32, 1135-1138.

European Medicines Agency, 2007. *European Pharmacopoeia* 6.0, pp. 287.

Ganderton, D., 1992. The generation of respirable clouds from coarse powder aggregates. *J. Biopharm. Sci.* 3, 101-105.

Geldart, D., 1973. Types of Gas Fluidization. *Powder Technology* 7, 285-292.

Grasmeijer, F., Lexmond, A.J., van der Noort, M., Hagedoorn, P., Hickey, A., Frijlink, H.W., De Boer, A.H., 2014. New mechanisms to explain the effects of added lactose fines on the dispersion performance of adhesive mixtures for inhalation. *PLOS One* 9, 1-11.

Guchardi, R., Frei, M., John, E., Kaerger, J.S., 2008. Influence of fine lactose and magnesium stearate on low dose dry powder inhaler formulations. *International Journal of Pharmaceutics* 348, 10-17.

Guenette, E., Barrett, A., Kraus, D., Brody, R., Harding, L., Magee, G., 2009. Understanding the effect of lactose particle size on the properties of DPI formulations using experimental design. *International Journal of Pharmaceutics* 380, 80-88.

Huck, D., 2007. Image Analysis Coupled with Classification – A Powerful Combination for the Study of Agglomeration. *Powder* 19, 42-44.

Jones, M.D., Price, R., 2006. The influence of fine excipient particles on the performance of carrier-based dry powder inhalation formulations. *Pharmaceutical Research* 23, 1665-1674.

Karhu, M., Kuikka, J., Kauppinen, T., Bergström, K., Vidgren, M., 2000. Pulmonary deposition of lactose carriers used in inhalation powders. *International Journal of Pharmaceutics* 196, 95-103.

Kinnunen, H., Hebbink, G.A., Peters, H., Shur, J., Price, R., 2014. Defining the critical material attributes of lactose monohydrate in carrier based dry powder inhaler

formulations using artificial neural networks. AAPS PharmSciTech Accepted manuscript.

Kinnunen, H., Shur, J., Hebbink, G.A., Muresan, A.S., Edge, S., Price, R., 2009. Spectroscopic Investigations into the Structure of Carrier-Based Dry Powder Inhaler Formulations Drug Delivery to the Lungs 20. The Aerosol Society, Edinburgh, pp. 120-123.

Kubavat, H.A., Shur, J., Ruecroft, G., Hipkiss, D., Price, R., 2012. Influence of primary crystallisation conditions on the mechanical and interfacial properties of micronised budesonide for dry powder inhalation. International Journal of Pharmaceutics 430, 26-33.

Louey, M., D., Razia, S., Stewart, P.J., 2003. Influence of physico-chemical carrier properties on the in vitro aerosol deposition from interactive mixtures. International Journal of Pharmaceutics 252, 87–98.

Louey, M., D., Stewart, P.J., 2002. Particle Interactions Involved in Aerosol Dispersion of Ternary Interactive Mixtures. Pharmaceutical Research 19, 1524-1531.

Lucas, P., Anderson, K., Staniforth, J.N., 1998. Protein deposition from dry powder inhalers: Fine particle multiplets as performance modifiers. Pharmaceutical Research 15, 562-569.

Marple, V.A., Roberts, D.L., Romay, F.J., Miller, N.C., Truman, K.G., Van Oort, M., Olsson, B., Holroyd, M.J., Mitchell, J.P., Hochrainer, D., 2003. Next Generation

Pharmaceutical Impactor (A New Impactor for Pharmaceutical Inhaler Testing). Part I: Design. *Journal of Aerosol Medicine* 16, 283-299.

Rogueda, P.G.A., Price, R., Smith, T., Young, P.M., Traini, D., 2011. Particle synergy and aerosol performance in non-aqueous liquid of two combinations metered dose inhalation formulations: An AFM and Raman investigation. *Journal of Colloid and Interface Science* 361, 649-655.

Šašić, S., Harding, L., 2010. Global illumination Raman chemical imaging of a combination of two drug molecules in a dry powder inhaler formulation. *Analytical Methods* 2, 1528-1535.

Shur, J., Harris, H., Jones, M.D., Kaerger, J.S., Price, R., 2008. The role of fines in the modification of the fluidization and dispersion mechanism within dry powder inhaler formulations. *Pharmaceutical Research* 25, 1931-1940.

Srichana, T., Brain, A., Martin, G.P., Marriott, C., 1998a. The determination of drug-carrier interactions in dry powder inhaler formulations. *Journal of Aerosol Science* 29, Supplement 2, S757-S758.

Srichana, T., Martin, G.P., Marriott, C., 1998b. On the relationship between drug and carrier deposition from dry powder inhalers in vitro. *International Journal of Pharmaceutics* 167, 13–23.

Steckel, H., Markefka, P., teWierik, H., Kammelar, R., 2006. Effect of milling and sieving on functionality of dry powder inhalation products. *International Journal of Pharmaceutics* 309, 51-59.

Steele, D., Young, P., Price, R., Smith, T., Edge, S., Lewis, D., 2004. The potential use of raman mapping to investigate in vitro deposition of combination pressurized metered-dose inhalers. *The AAPS Journal* 6, 41-44.

Susi, H., Ard, J.S., 1974. Laser-raman spectra of lactose. *Carbohydrate Research* 37, 351-354.

Thalberg, K., Berg, E., Fransson, M., 2012. Modeling dispersion of dry powders for inhalation. The concepts of total fines, cohesive energy and interaction parameters. *International Journal of Pharmaceutics* 427, 224-233.

Theophilus, A., Moore, A., Prime, D., Rossomanno, S., Whitcher, B., Chrystyn, H., 2006. Co-deposition of salmeterol and fluticasone propionate by a combination inhaler. *International Journal of Pharmaceutics* 313, 14-22.

Willen, U., 2008. Automation in image analysis for particle size and shape measurement. *G.I.T. Laboratory Journal* 7-8, 34-36.

Young, P.A., Edge, S., Traini, D., Jones, M.D., Price, R., El-Sabawi, D., Urry, C., Smith, C., 2005. The influence of dose on the performance of dry powder inhalation systems. *International Journal of Pharmaceutics* 296, 26-33.

Tables

Table I Average proportion of fines below 4.5 μm in the lactose carriers ($\% < 4.5 \mu\text{m}$, $n=5$) and summary of *in vitro* performance of budesonide formulations prepared with the carriers in terms of fine particle fraction of emitted dose (FPF_{ED}) and mean mass aerodynamic diameter (MMAD). The data for FPF_{ED} and MMAD represents mean \pm standard deviation, $n=3$.

	% < 4.5 μm	$\text{FPF}_{\text{ED}} \pm$ S.D. (%)	MMAD \pm S.D. (μm)
LH100	1.29	24.10 \pm 0.24	2.58 \pm 0.02
+20% LH210	6.02	26.63 \pm 0.13	3.14 \pm 0.01
+20% LH300	23.04	39.74 \pm 1.34	3.36 \pm 0.03

Table II The 10th, 50th and 90th percentiles of number based and volume converted circular equivalent (CE) diameter distributions and mean values of high sensitivity (HS) circularity and convexity of material collected on Stage 2 of the Next Generation Impactor

	Number based particle size (μm)			Volume converted particle size (μm)			Particle shape Mean values	
	d_{10}	d_{50}	d_{90}	d_{10}	d_{50}	d_{90}	HS Circularity¹	Convexity²
LH100	1.56	3.84	5.77	3.68	5.35	8.06	0.859	0.986
+20% LH210	1.72	3.62	6.14	3.60	5.98	9.48	0.846	0.983
+20% LH300	1.86	3.94	6.72	3.95	6.53	10.4	0.824	0.980

1 Convexity is calculated as convex hull diameter of a particle divided by the actual perimeter of the particle

2 High sensitivity (HS) circularity is calculated as 4π times the area of the particle over perimeter squared

Table III Proportions of budesonide, lactose and agglomerates of the two species deposited on Stage 2 of the Next Generation Impactor from the different formulations aerosolised on Cyclohaler at 90 l/min. The data are based on Raman analysis of 1353 (LH100), 1095 (+20% LH210) and 1156 (+20% LH300) particles collected on a microscope slide placed on Stage 2.

	Lactose (%)	Budesonide (%)	Agglomerates (%)
LH100	37.4	48.8	13.8
+20% LH210	79.0	9.5	11.5
+20% LH300	77.3	5.7	17.0

Table IV The mean \pm standard deviation (n=3) amount of budesonide recovered from Stage 2 of the Next Generation Impactor, total proportion of species containing budesonide of the particles analysed by Raman for each of the formulations and the amount of pure budesonide and budesonide in agglomerates on Stage 2 based on the Raman analysis.

	Budesonide on Stage 2 \pm S.D. (μg)	Total budesonide (%)	Pure budesonide (μg)	Budesonide in agglomerates (μg)
LH100	3.37 \pm 0.10	62.6	2.6	0.7
+20% LH210	4.78 \pm 0.10	21.0	2.2	2.6
+20% LH300	9.82 \pm 0.14	22.7	2.4	7.4

Figures

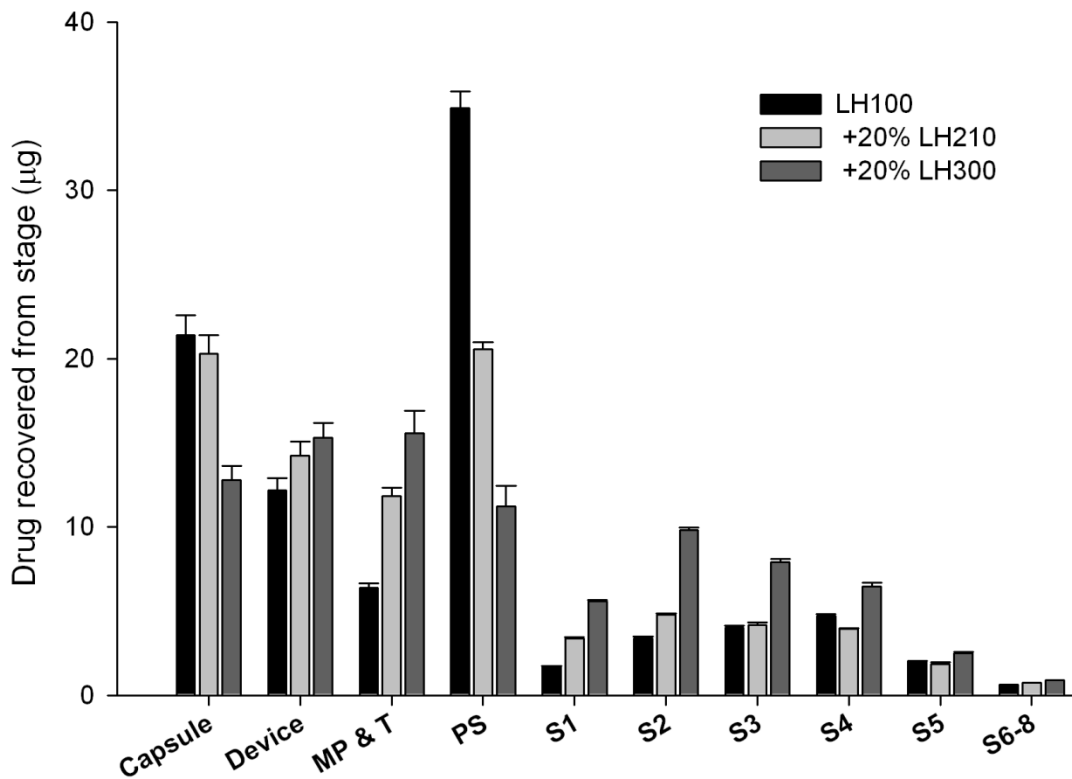


Figure 1. Stage-by-stage deposition profile of micronised budesonide within the Next Generation Impactor from model formulations prepared with LH100 (black bars), 20% LH210 in LH100 (light grey) and 20% LH300 in LH100 (dark grey) as carriers and aerosolised using a Cyclohaler device at 90 l/min. The error bars represent standard deviation, n=3. MP & T is mouthpiece and throat, PS is pre-separator and S denotes stage. Stages 6-8 are grouped together for clarity of presentation.

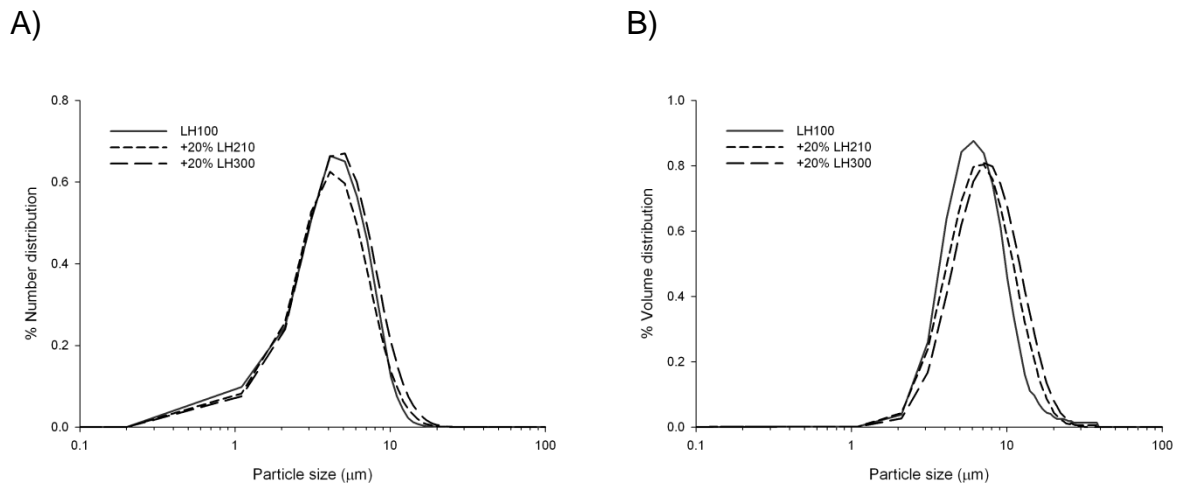


Figure 2. A) number based and B) volume converted circular equivalent (CE) diameter distributions of particles collected on a microscope slide placed on Stage 2 of the Next Generation Impactor from formulations prepared with LH100 (solid line), 20% LH210 in LH100 (short dash) and 20% LH300 in LH100 (long dash) as carrier for micronised budesonide aerosolised at 90 l/min on a Cyclohaler.

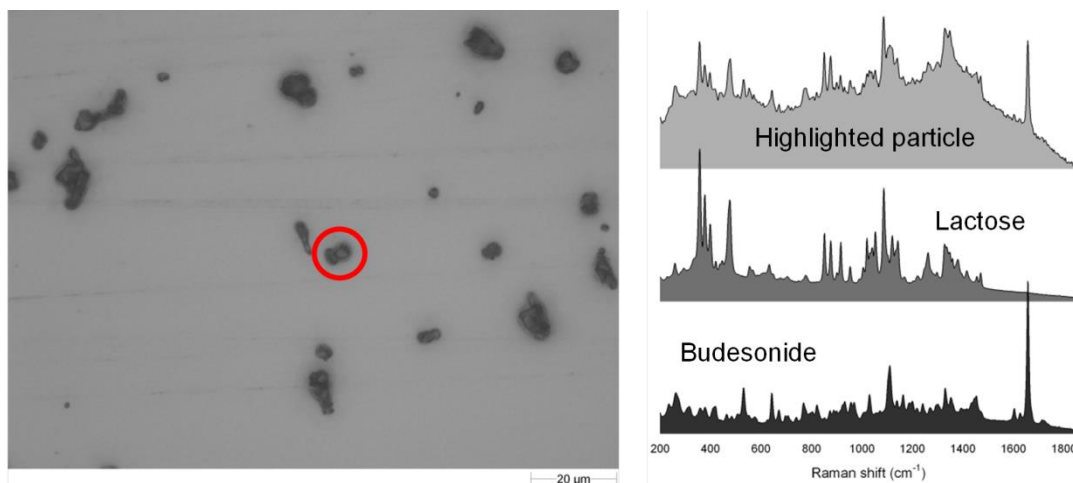


Figure 3. A 50x magnification field of view photomicrograph of particles deposited on Stage 2 of the Next Generation Impactor (left), the Raman spectra of the highlighted particle (top right) and the library spectra of α -lactose monohydrate (middle right) and budesonide (bottom right)

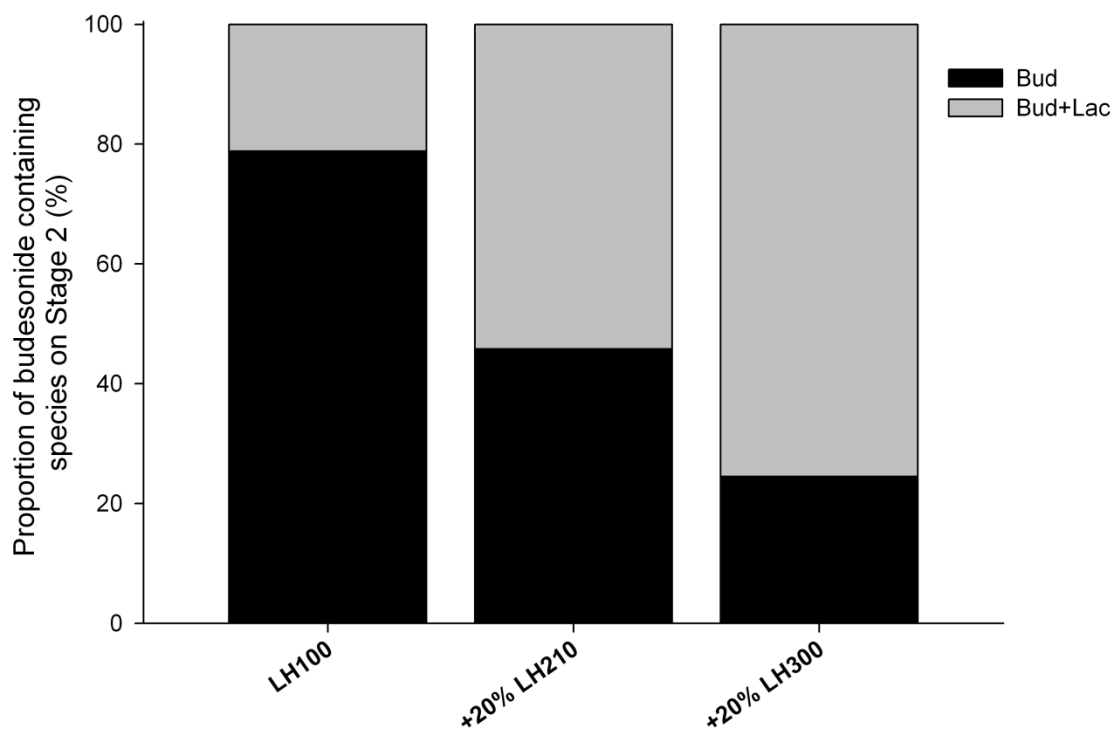


Figure 4. Proportions of pure budesonide (black) and the agglomerates of budesonide and lactose (grey) of the budesonide containing species collected on Stage 2 of the Next Generation Impactor when aerosolised from the formulations of micronised budesonide with LH100 (left), 20% LH210 in LH100 (middle) and 20% LH300 in LH100 (right) and as characterised by the Raman fingerprint of the particles